



# The Development of a Refined Printing System For Metal/Ceramic Composite Materials

K MAHADEVASWAMY <sup>1</sup>, SANGEETHA S A <sup>2</sup>

<sup>1</sup> Senior Scale Lecturer, Department of Mechanical Engineering (HPT), S J (Government) polytechnic Bengaluru, Karnataka, India.

<sup>2</sup> Senior Scale Lecturer, Department of Ceramics Technology, S J (Government) polytechnic Bengaluru, Karnataka, India.

---

## Abstract

The process of additive manufacturing for ceramic/metal composites merges the inherent benefits of these materials with the versatility of 3D printing, facilitating the tailored creation of intricate structures and promoting advancements in lightweight design solutions. This technology is presently utilized across various sectors, including aerospace and automotive, for the processing and manufacturing of high-performance components. In this investigation, we devised a material extrusion 3D printing apparatus for the fabrication of metal-ceramic hybrid structures. The system enables low-heat printing, allowing for the straightforward and secure debinding of printed samples through an alcohol-based method, thereby streamlining the process flow and enhancing the processing efficiency of high-performance composites. Moreover, this research involved the development of 3D printed composites of SUS316L/ZrO<sub>2</sub> to create complex structural components.

**Keywords:** Ceramic/Metal Composites; 3D Printing; Low-Heat Printing.

---

## I. INTRODUCTION AND LITERATURE REVIEW

Ceramics are a material that is appealing for use in a variety of structural components because of its exceptional high-temperature capabilities, resilience to wear, and resistance to corrosion (1,2). Zirconia, in particular, is a significant ceramic material that has features such as high stability at high temperatures, high bending strength and fracture toughness, and biocompatibility 3,4. On the other hand, ceramics are difficult to work with because of their low machinability and brittleness, which makes it difficult to manufacture big and complicated structures, which in turn limits their applicability. The technique that allows metal and ceramics to be joined together has thus garnered a lot of interest. Through the process of connecting metal and ceramics, it is possible to increase material qualities that cannot be reached by a single material. This opens the door to a broad variety of applications. The development of a 3D printing technology that is capable of producing hybrid constructions made of ceramics and metals is one of our primary goals. There is a significant amount of use of metal and ceramic in the construction of structural materials (6-7), oxygen sensors (9-11), and solid oxide fuel cells (SOFCs) (12-15). The technologies of welding, brazing, and diffusion bonding are used often in the process of uniting metals and ceramics. There are, however, certain downsides associated with these approaches, such as the need for extra procedures or materials in order to link. Therefore, it is desirable to have manufacturing methods that do not call for any extra operations to be performed in order to link.

The purpose of this research was to design a dispenser-based metal 3D printing technology that allows for printing with low heat and easily debinding the material. As the printing medium, we make use of a newly developed compound material that is comprised of zirconia powder and stainless steel powder that have been combined with a thermoplastic binder. In a manner that is analogous to the powder metallurgy process, the printed samples are debound and sintered. However, the debinding process may be carried out in a secure manner by using alcohol, and it does not need the use of sophisticated apparatus. Using the 3D printing method that we have created, we also make an effort to print hybrid structures made of ceramic and stainless steel, and we examine the interface via the process of co-sintering. The use of this process makes it possible to include ceramics that are resistant to corrosion and have a high level of hardness with metal components in order to create composite materials. Additionally, components that have three-dimensional ceramic structures inside them are shown, and we show that the areas that include ceramics have a greater level of hardness.

## II. PRINTING SETUP

### 2.1 Material

A brand new substance that could be printed at a much lower temperature of roughly 80 degrees Celsius was created as part of this research project. Rapeseed oil, a synthetic wax thermoplastic resin (PALVAX, Nippon Seiro Co., Ltd.), and stearic acid were the other components that went into the production of the binder. In order to complete the preparation of the binder, these components were combined, then heated in a microwave until the synthetic wax was completely dissolved in the rapeseed oil while being stirred. The gelatinization of the rapeseed oil was accomplished with the aid of stearic acid, which not only assists in maintaining the shape of the printed sample but also assists in the uniform dispersion of the combined metal and ceramic powders.

The compound was then made by incorporating metal or ceramic powder into the binder, heating the mixture to 80 degrees Celsius in an oven, and stirring it using a planetary mixing equipment (SK-350T, Shashin Kagaku Co., Ltd.). This process followed the preparation of the compound. This research used powder materials consisting of stainless steel powder (SUS316L, Daido Steel Group) with an average particle size of about 10  $\mu\text{m}$  and zirconia powder (TZ-3Y-E, Tosoh Corporation) with a particle size of 40 nm. Both of these powder materials were utilized for investigation purposes. In accordance with the above description, the binder was produced by combining rapeseed oil, synthetic wax, and stearic acid in a mass ratio of 89:9:2, respectively. During the printing process, the powder and the binder were combined at a volume ratio of one to one.

### 2.2 3D Printing System

In order to execute 3D printing, one must acquire data that delineates the trajectory of the print by segmenting the 3D model into discrete layers. To achieve this objective, we employed a slicer software (PrusaSlicer, Prusa Research) that is widely utilized for resin filament 3D printers. Furthermore, the control software for the dispenser device (MuCAD, Musashi Engineering, Inc.) was employed for the printing processes utilized in this study. The G-code program generated by the slicer software was translated into the code for the dispenser control system through our custom-developed Python program.

Figure 1(a) illustrates the three-dimensional printing apparatus employed in this investigation. A dispenser device, specifically the SHOTMASTER 300SX from Musashi Engineering, Inc., served as the apparatus for 3D printing. This printing system is capable of producing a three-dimensional pattern by maneuvering the stage along the y-axis while simultaneously adjusting the dispenser along the x- and z-axis directions. Furthermore, the material underwent extrusion via an air pulse type dispenser (ML-5000XII, Musashi Engineering, Inc.), facilitating the concurrent regulation of the dispenser's coordinates, movement velocity, and the extrusion pressure of the compound. Additionally, given that the printing material in this investigation necessitates heating, two ceramic heaters were affixed to the nozzle component, while a silicone rubber heater was secured to the syringe section. The temperature was meticulously regulated at 80 °C utilizing a digital fine thermo (DG2N, Hakko Electric). The composite substance underwent heating in an oven at a temperature of 80 °C prior to being introduced into the syringe for the printing process. The syringe containing the substance was subsequently heated to 80 °C and affixed to the printing apparatus. The substance within the syringe was subjected to pressure by the dispensing apparatus and was subsequently ejected through a nozzle measuring 0.50 mm in diameter. Printing was conducted on an alumina board secured to the stage, and in accordance with the established printing program, the compound was inscribed as the process advanced.

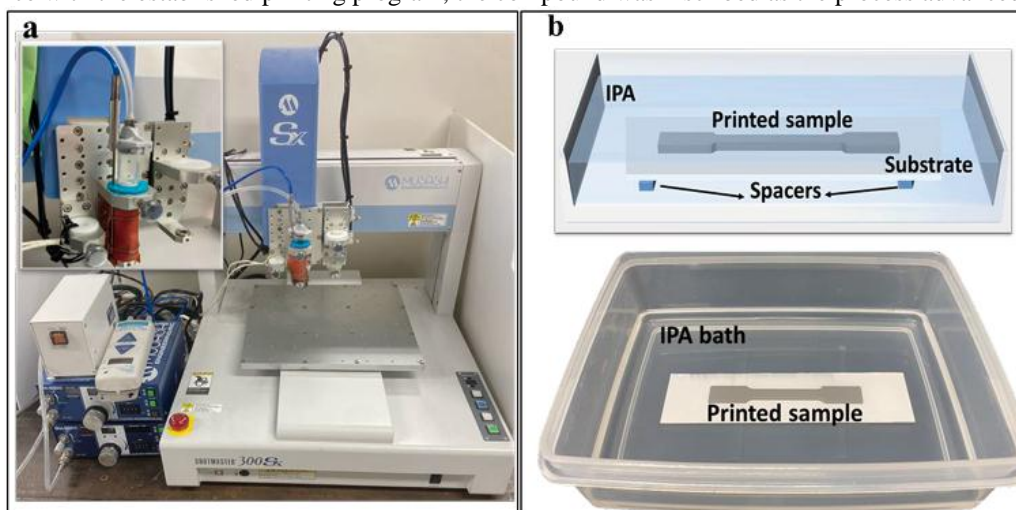


Fig .1. (a) 3D printing system, (b) Degreasing system.

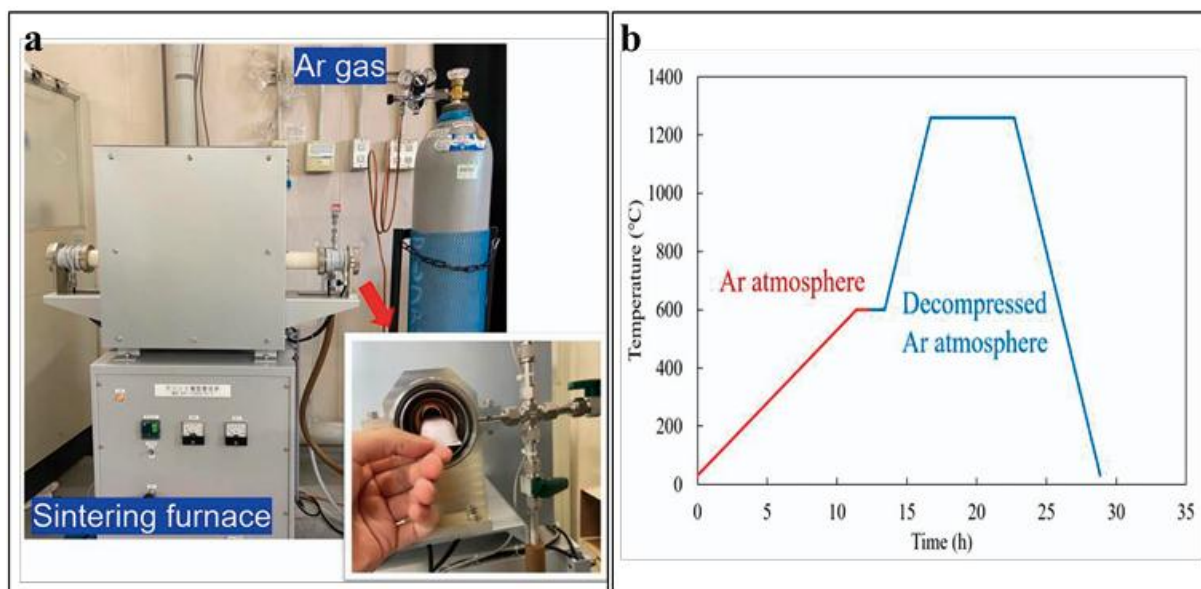


Fig.2. (a) Sintering system, (b) Variation of sintering temperature

### 2.3 Debinding and Sintering

Typically, the process of solvent debinding necessitates the use of specialized equipment and hazardous solvents. However, in this study, the binder prepared can be effortlessly debound by immersing the sample in an isopropyl alcohol (IPA) bath, eliminating the need for any specialized apparatus. The printed sample was maintained at room temperature in the bath for approximately 86 ks (1 day), as illustrated in Fig. 1.(b). Throughout this period, the predominant component of the binder, rapeseed oil, was dissolved and subsequently eliminated by the IPA. Conversely, the synthetic wax present in the binder exhibited insolubility in IPA, thereby preserving the integrity of the printed sample's shape. In order to avert the accumulation of the extracted rapeseed oil at the base of the IPA bath, which could obstruct the solvent debinding procedure, spacers were strategically positioned beneath the alumina board supporting the sample. The debound sample underwent sintering in an electric furnace. This investigation employed a horizontal tube furnace equipped with molybdenum silicide heaters (HF-1500-S-T, Crystal Systems Co., Ltd.) for the sintering process, as illustrated in Fig. 2.(a). The furnace was linked to an argon gas cylinder and a vacuum pump to regulate the sintering environment. The samples, having undergone solvent degreasing, were positioned at the center of the tubular furnace for the sintering process to take place. Figure 2(b) illustrates the temperature and atmospheric conditions present during the sintering process. Prior to the main analysis, a sequence of initial assessments was carried out to ascertain the requisite conditions. Initially, the sample underwent heating to 600 °C at a rate of 50 °C/h within an argon atmosphere, maintained for a duration of 7.2 ks (2 hours). Throughout this procedure, the residual binder within the sample was eliminated through the method of thermal decomposition. During this period, as the adhesion between the metal and ceramic powders was advancing, the form remained intact even following the elimination of the binder. Subsequently, the environment was altered to a low-pressure argon setting (ranging from 1 kPa to 100 kPa), and the specimen was elevated to a temperature of 1350 °C at a rate of 200 °C/h, maintained for a duration of 21.6 ks (6 h) to facilitate the bonding of the powder particles and enhance the density of the sample. The sample was subsequently cooled to room temperature at a rate of 200 °C/h.

## III. RESULTS AND DISCUSSION

### Metal-Ceramics Hybrid Structures

Through the use of MIX compound and stainless steel compound, we were able to create a hybrid construction. Mix compounds were created by combining powders of zirconia and stainless steel in four distinct volume ratios: 45:55, 50:50, 55:45, and 60:40 according to the volume ratio. The composition of the binder and the procedure used to prepare the Mix compound were identical to those described in the preceding section. The first thing that we did was print a composite construction utilizing Mix and compounds made of stainless steel. Figure 3 illustrates the structure of each layer in the structure. There were seven layers of a square with a side of 18 millimeters that were printed using stainless steel compound. Mix compound was printed within the square in a serpentine pattern. The total construction comprised of these seven layers. In order to print the first and second layers, a square of stainless steel compound was used. After leaving a route for printing Mix compound, the third layer was printed with stainless compound before printing Mix compound. This completed the printing process. The fourth layer was printed using a square of stainless steel compound as the printing medium. Before



beginning the printing process, we rotated the structure of the third layer by ninety degrees in preparation for the fifth layer. The sixth and seventh layers were printed using a composition made of stainless steel.

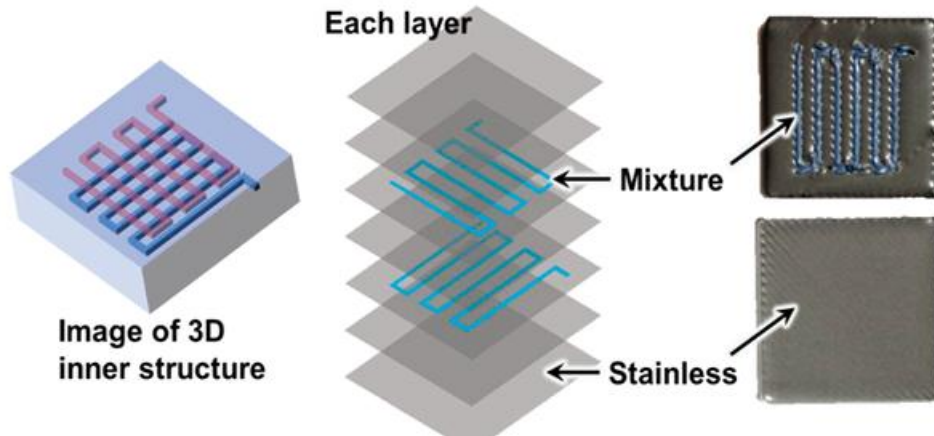


Fig.3. The structure printed on each layer and the actual printed sample

The samples that were sintered are shown in Figure 4 (a-1) through (d-1). In the samples, warping was seen following the sintering process. In the Mix compound, the sample that had the largest volume ratio of stainless steel, which was 60:40, displayed the least amount of warping during the course of the experiment. When it comes to the quantity of shrinkage that occurs during the sintering process, the Mix and stainless steel compounds would be subject to different levels. It is also hypothesized that the warping in the form of a horse's saddle was caused by the change in orientation of the third and fifth layers, which was three hundred and ninety degrees. In addition, a picture captured by an optical microscope of the interface area associated with each sample is shown in Figure 8. In the equation  $(a-2)^{(d-2)}$ , the component made of stainless steel is shown in orange, while the part made of zirconia is described in gray. A huge gap was detected at the interface of the two samples that included a low fraction of stainless steel. This gap appeared as a black section for the purpose of observation.

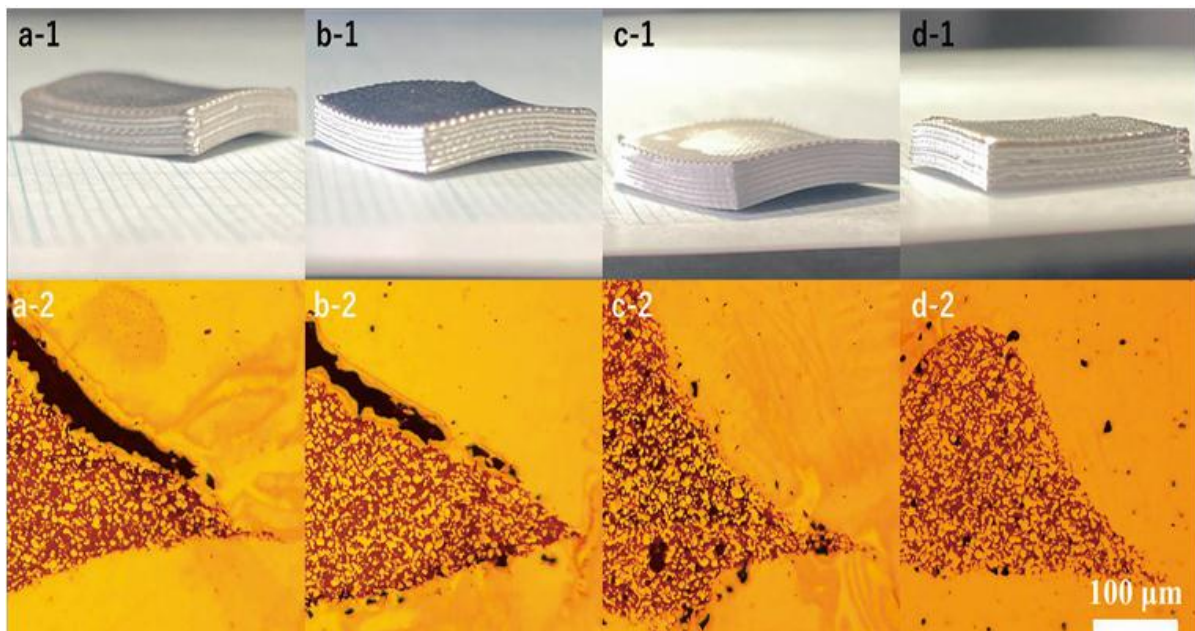
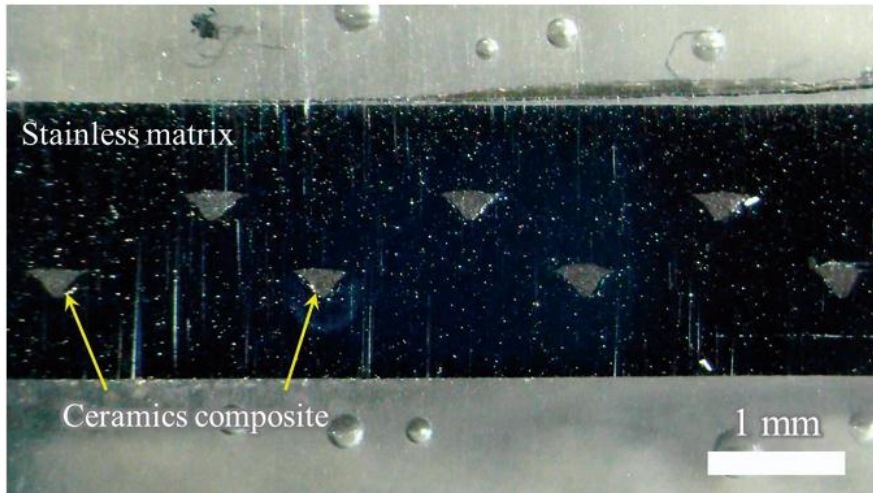


Fig.4. Samples after sintering

The cross-sections of four samples were inspected after they were cut into two pieces and then passed through the corners of a square via the process of cutting. In Figure 5, the view of the cross-section is shown. The zirconia-containing area was distributed in a regular pattern, and the form of the cross-section might be described as triangular. The findings of the line scan performed by EDS analysis are shown in Figure 6, along with the cross-sectional SEM picture of the sample that was created using the 60:40 Mix compound. The regions of the SEM picture that are black are representative of stainless steel, while the areas that are brilliant

are representative of zirconia. In the zirconia component of the Mix compound, it was noticed that there were many holes not exceeding 5  $\mu\text{m}$  in size. At the interfaces between the metal and the ceramic, however, a good joint was produced that did not include any gaps. Within the interface, the line scan analysis revealed the presence of iron (Fe) and zirconium (Zr), and it was discovered that there was a diffusion phase of roughly 1  $\mu\text{m}$ . Additionally, this finding demonstrates that the materials have a good interaction.



**Fig.5.** Stereomicroscopic image of the cross section and optical microscopic image of the junction surface of the stainless steel layer and the mix layer

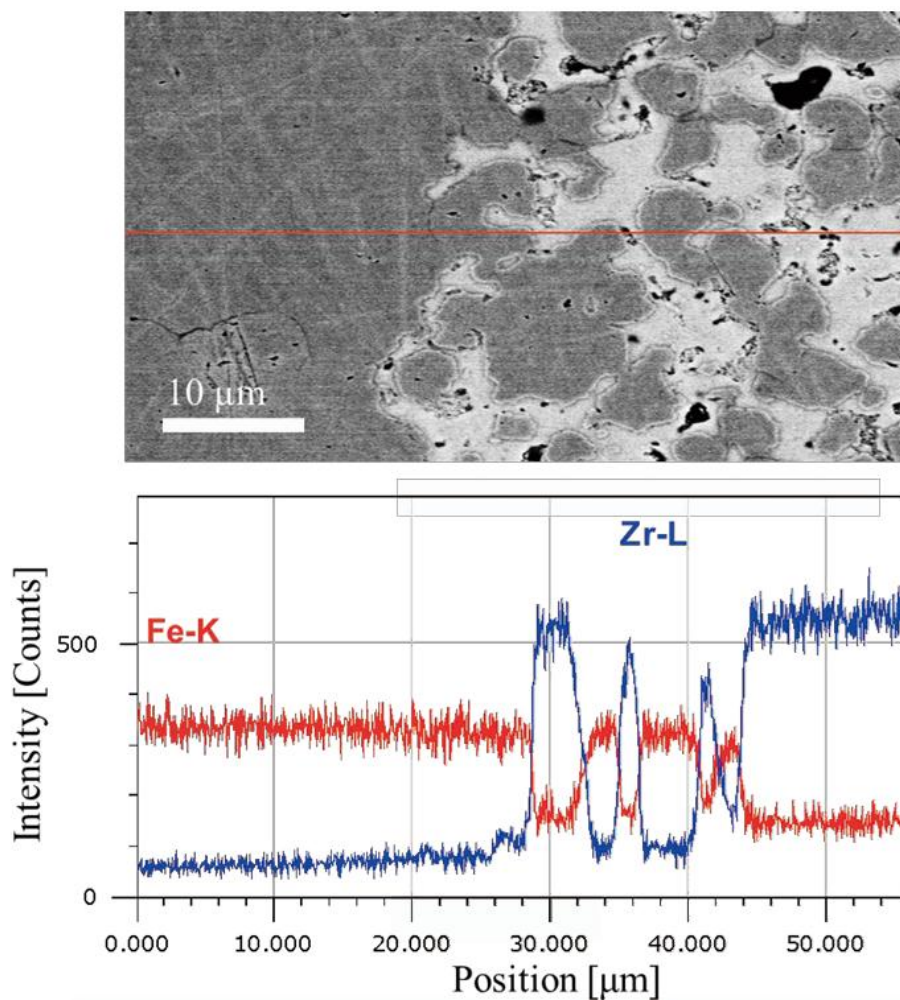


**Fig.6.** Results of SEM image and EDS analysis of the interface of the sample 4 between stainless steel and mixture

#### **IV. CONCLUSION**

A novel compound has been synthesized that enhances the process of low-temperature 3D printing and simplifies the debinding procedure. Furthermore, we developed a material extrusion 3D printing system utilizing this compound. Employing our advanced system, we fabricated hybrid structures using stainless steel powder and zirconia powder, successfully attaining high-density samples via co-sintering. The novel compound, consisting of rapeseed oil, synthesized wax, and stearic acid, demonstrated efficacy in facilitating solvent debinding through the utilization of an IPA bath. Furthermore, we achieved the successful fabrication of a metal-ceramic hybrid structure through the amalgamation of stainless steel and zirconia with the compound, culminating in a sintered body that exhibited no complications. The achievement of co-sintering metals and ceramics via 3D printing represents a noteworthy advancement, considering the complexities inherent in this process.

Moreover, the significant hardness exhibited in the ceramic areas indicates promising applications, including the production of mechanical components that possess improved wear resistance on their surfaces. Consequently, this technology presents a compelling approach for the fabrication of hybrid structures comprising metal and ceramics, showcasing potential applications that capitalize on the advantageous characteristics inherent to both materials.

#### **REFERENCES**

- [1]. J.-M. Schneider, et al.: *Materials Science and Engineering: A*, 262 (1999), 256-263.
- [2]. A. Ruh, et al.: *International Journal of Applied Ceramic Technology*, 8(2011), 194-202.
- [3]. M. Dourandish, et al.: *Journal of the American Ceramic Society*, 91 (2008), 3493-3503.
- [4]. U. Betz, et al.: *Materials Science and Engineering: A*, 281(2000), 68-74.
- [5]. C.W. Gal, et al.: *International Journal of Applied Ceramic Technology*, 16(2019), 315-323.
- [6]. A. Marocco, et al.: *Solid state sciences*, 14(2012), 394-400.
- [7]. J. Bauer, et al.: *Science Advances*, 8(2012), eabo3080.
- [8]. A. Katz-Demyanetz, et al.: *Manufacturing review*, 6 (2019), 5.
- [9]. N. Rajabbeigi, et al.: *Sensors and Actuators B: Chemical*, 100(2004), 139-142.
- [10]. B. Elyassi, et al.: *Sensors and Actuators B: Chemical*, 103(2004), 178-183.
- [11]. N. Rajabbeigi, et al.: *Sensors and Actuators B: Chemical*, 108(2005), 341-345.
- [12]. J.W. Fergus: *Journal of Power Sources*, 147(2005), 46-57.
- [13]. R.N. Singh: *International Journal of Applied Ceramic Technology*, 4(2007), 134-144.
- [14]. R.N. Singh: *Journal of Materials Research*, 27(2012), 2055-2061.
- [15]. Xu Y, et al.: *Micro & Nano Letters*, 8(2013), 571-574.